FLUID MOTION OVER SUCCESSIVE SQUARE PROTUBERANCES MOUNTED ON A FLAT PLATE: FLOW PATTERNS AND VORTEX SHEDDING FREQUENCY

Giulio Dalmolin Cervo, giuliocer@aluno.feis.unesp.br
Fábio Basaglia Fonseca, fabiobf88@gmail.com
Sérgio Said Mansur, mansur@dem.feis.unesp.br
Edson Del Rio Vieira, delrio@dem.feis.unesp.br
UNESP – Ilha Solteira, São Paulo, Brazil

Abstract. *In the present paper, flow patterns and vortex shedding phenomenon produced by square protuberances placed on a smooth flat wall are experimentally studied by means of flow visualization and hot-film anemometry. Qualitative and quantitative information have been obtained for Reynolds numbers up to 2500. The experiments have been performed in a vertical low turbulence hydrodynamic tunnel operated by gravitational action in blow-down mode. Flow patterns have been captured in photographic still images, while vortex shedding frequencies have been determined by hot-film anemometry. Injection of liquid dye upstream protuberances have allowed to visualize the recirculating flow inside cavities as well as vortex formation and shedding in the shear layer over the protuberances. Flow visualization has also helped to identify the best position to insert the hot-film probe in the flow in order to obtain a vortex shedding frequency with a high signal noise ratio. Flow visualization images obtained at different Reynolds have shown the complex topological structure of the flow, characterized by vortex shedding, recirculating bubbles, reverse flow and boundary layer separation and attachment. Additionally, the behavior of the dimensionless vortex shedding frequency as a function of the Reynolds number has been determined.*

Keywords*: Flow visualization, Vortex shedding .*

1. INTRODUCTION

Rough surfaces immersed in a flow are often used in engineering to increase the performance of thermal and hydraulic equipment. Flow over rough walls has two important parameters: the roughness Reynolds number, k_s, which measures the effect of the roughness in the buffer layer, and the ratio of the boundary layer thickness to the roughness height (Jiménez, 2004). Under a hydrodynamic point of view, two classes of roughness surface can be identified. In the first one, known as K type, the roughness Reynolds number, k_s, should be proportional to the dimensions of the roughness elements and also has recirculation bubbles that reattach ahead of the next rib, exposing it to the outer flow, as illustrated in Fig. 1(b). K type roughness act as turbulence promoters and can be frequently found in separators, filters and plate heat exchangers. In electronic systems, the roughness surfaces are formed by electronic components, whose disposition strongly affects the fluid motion and heat dissipation. Thus the shapes and positions of the components should be carefully chosen in order to keep the temperature in acceptable levels. For this, the flow characteristics must be well known.

The second type of roughness, known as D type, the effective roughness is not proportional to the roughness height, but to the boundary layer thickness. The grooves in D type wall sustain stable recirculation vortices that isolate the outer flow from the roughness, as showed in Fig. 1(a).

In this present work, the configuration of the flow on a ribbed smooth flat wall, represented by square cylindrical protuberances equally spaced, is experimentally studied by means of flow visualization and hot film anemometry.

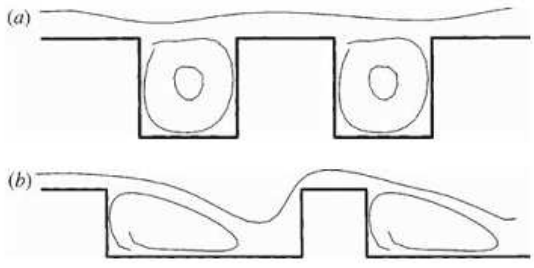

Figure 1. Geometry of (a) D type, and (b) K type walls. (Jiménez, 2004)

2. EXPERIMENTAL PROCEDURE

The experiments have been performed for Reynolds numbers up to 2500 in a low turbulence hydrodynamic tunnel

with a test section of 146×146×500 mm. The tunnel is operated by gravitational action in blow-down mode producing a low turbulence level (Bassan *et al.*, 2011). Fig. 2 shows the non perturbed free stream velocity and the velocity fluctuation in the test section where square protuberances are mounted on a flat plate, as illustrated in Fig. 3.

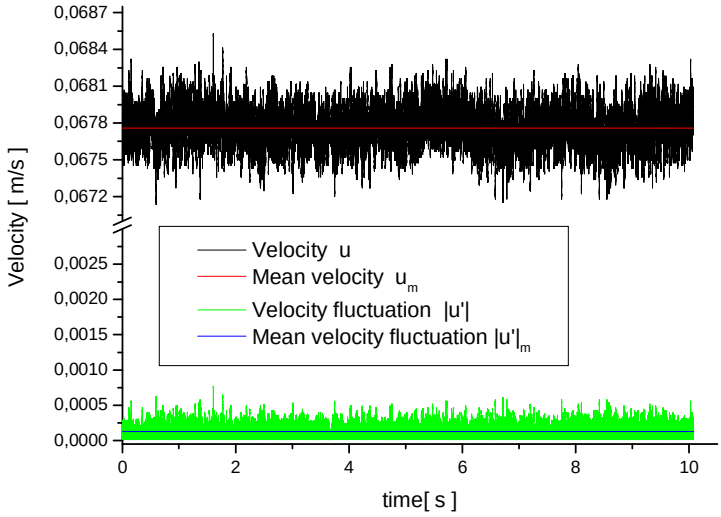

Figure 2. Free stream velocity and velocity fluctuation in test section.

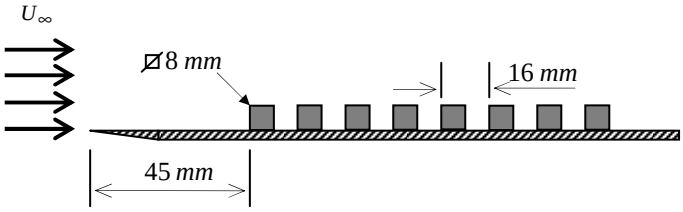

Figure 3. Smooth flat plate with square protuberances.

The flow visualization technique is the direct injection of opaque liquid dye in non-perturbed flow by means a long hypodermic needle of 0.7 mm O.D. A solution of PVA pigments, tap water and ethyl alcohol has been used as dye. Small quantity of ethyl alcohol is used only to control the dye density keeping it close to water density utilized in the tests. Sufficient amount of dye has been injected directly in the non-perturbed stream, to color the entire flow field. Subtly, the injection dye stopped and the clean water flow wash the entire flow field, except the recirculation between each protuberance and the wake, because in these regions the flow speed is significantly small than in other ones. This procedure permits to see, for some few seconds, the recirculating regions and the wake downstream the protuberances. More details on flow visualization techniques by means of liquid dye injection can be found in Clayton and Massey (1967), Freymuth (1993) and Merzkirch (1987).

Still images have been captured using a D 90 Nikon DSLR camera with a Nikkor 120 mm macro lens. Cold illumination by means of fluorescent lamps with high color temperature, but minimal heat emission, has been adapted in the tunnel allowing sharp and well defined images. The use of Rosco color illuminating filter Cinegel#3308 converts daylight fluorescent lamps to 5500 K and a diffuser Cinegel#3007, a slight filter with less density softens edge and provides a good illumination for still and video image capture.

Velocity measurements have been performed with 55R11 and 55R15 probes made by Dantec Measurement Technology. This is a straight general-purpose type sensor which permits a wide measurement range in water medium. For very small velocities several special cares could be adopted in order to reduce the convection effect around the probe. Indeed, a hot-film probe immersed in recirculation zones can produce a high level of thermal convection interfering in the measurements. Hot-film measurements over the protuberances were employed to obtain temporal flow velocities. Data acquired by hot-film probe have been processed to obtain a frequency spectrum with FFT – Fast Fourier Transform.

3. RESULTS

Flow patterns at relatively low Reynolds number are presented in Fig. 4. Near creeping flow, there is a very little detachment with the dye streakline skirting almost perfectly solid obstacles - Fig. 4 (a).

Figure 4(b) shows one clockwise recirculation in each cavity for Reynolds number equal to 8. This occurs due to the difference in the mean flow velocity and the low velocity inside the cavities. It can also be seen the beginning of the recirculation bubble upstream the first protuberance. The shear layer is visualized in Fig. 4(c) and Fig. 4(d) for Reynolds number equal to 98 and 160, respectively. There is a decreasing process in the clockwise vortex size concomitantly with the appearance of a secondary counterclockwise vortex at the left bottom of the cavity. This is known because of the dye was "washed" by the flow, indicating that there is water movement in this region. The location of the detachment boundary layer points are similar and can be noted at the right top of the first protuberances. On the other hand, the attachment occurs in the left top of the following obstacles.

For Reynolds number equal to 228, Fig. 4(e), the mean vortex seems to be outside of the cavity and the detachment and attachment points are not easily recognized, except the first obstacle detachment point, which is nearest to the top left edge due to the velocity increase. Furthermore, the shear layer becomes thicker and the recirculation bubble upstream the first protuberance is clearly identified.

A different flow pattern occurs when Reynolds number gets equal to 445, Fig. 4(f), since there are two vortex regions which were not found for low Reynolds number. There is a counterclockwise vortex inside each cavity while a clockwise vortex appears over the protuberances. These vortex are formed due to the countercurrent flow which appears because there is a different pressure gradient inside the boundary layer. The beginning of Kelvin-Helmholtz instabilities is also recognized over the obstacles due to the different velocity gradient.

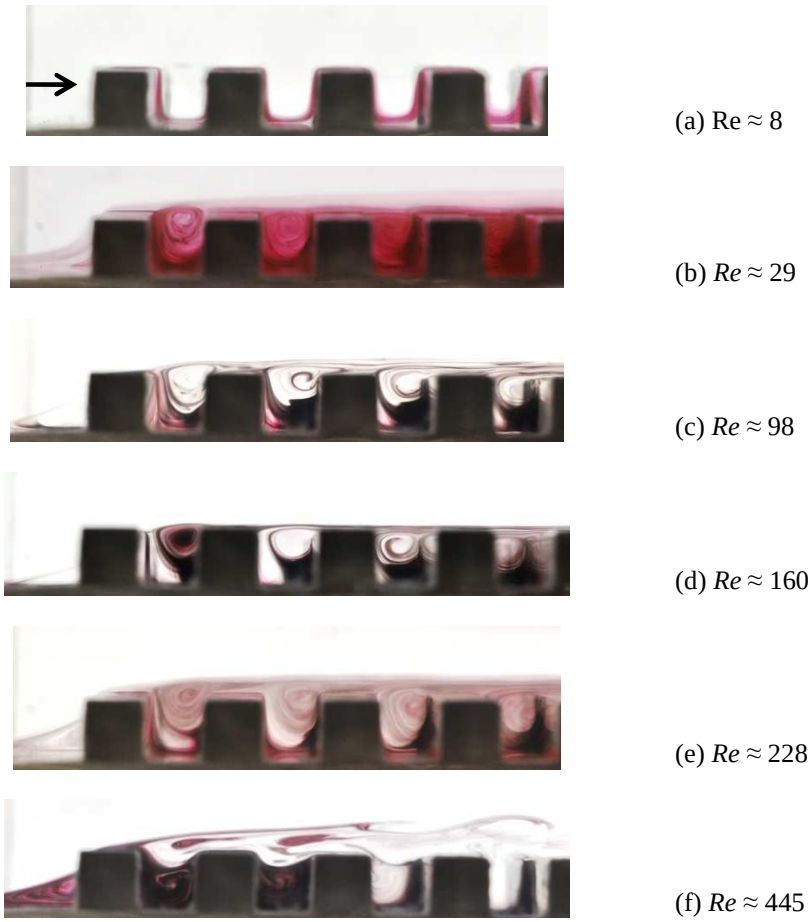

(a) Re ≈ 8

(b) *Re* ≈ 29

(c) *Re* ≈ 98

(d) *Re* ≈ 160

(e) *Re* ≈ 228

(f) *Re* ≈ 445

Figure 4. Flow visualized image for different Reynolds numbers.

The boundary layer detachment is shown in Fig. 5. All the images show the detachment point near the left edge of the first protuberance. Figure 5(a) shows the Kelvin-Helmholtz instabilities and the flow pattern is similar to the Fig. 4(f) however, the recirculations over the obstacles are "flattened" due to the velocity increase. It can also be seen that the vortex inside the first cavity has less kinetic energy, since the dye is initially "washed" in this cavity than the following ones. The Fig. 5(b) and Fig. 5(c) show the recirculation bubble upstream in the first protuberance. The instabilities, vortex shedding as well as the recirculations inside the cavities are hard to identify because of the high flow velocity which spreads the dye in a few seconds.

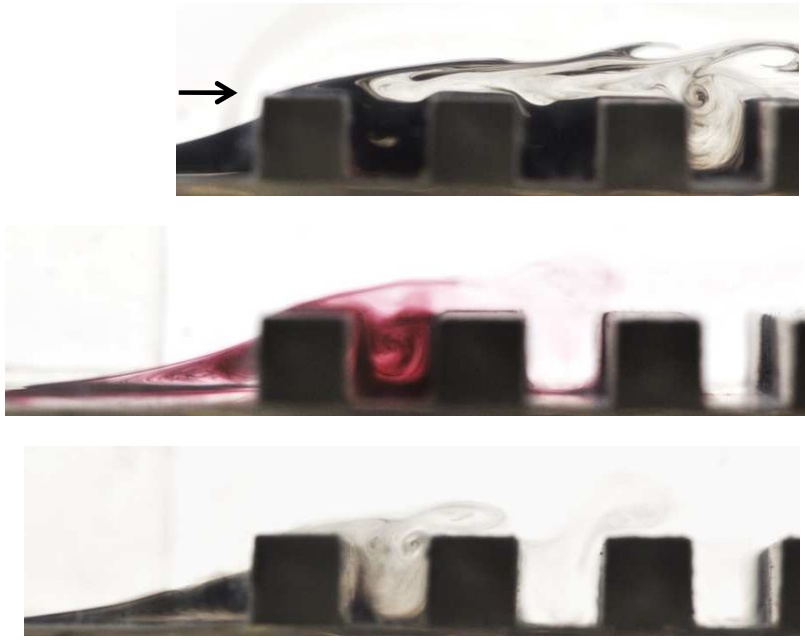

(a) $Re \approx 512$

(b) $Re \approx 860$

(c) $Re \approx 1010$

Figure 5. Boundary layer detachment and vortex structures visualization for different Reynolds numbers.

Figure 6 shows the Reynolds number versus Strouhal frequency, this curve was obtained from velocity signals, directly acquired in the flow by hot-film anemometry, and their corresponding FFT – Fig. 7. On the frequency spectrum curve, the highest peaks represent the Strouhal frequency. Figure 6 depicts a linear behavior from Reynolds number equal to 445 until Reynolds number equal to 1500. Note that there are two discontinuity regions for Reynolds numbers 1550 and 2000. This phenomenon probably occurs due to a different flow pattern. Fig. 7(f) shows two highest peaks which represent the vortex shedding frequency in discontinuity region. Note that the high and the low frequencies are present and probably they exist for others high Reynolds numbers, but usually one of them can be measured because of its higher amplitude. Unfortunately, due to the digital video camera`s limitation of 30 fps (frames per second), it was not possible to investigate the flow characteristics. At least a 150 fps digital video camera is necessary to study the instabilities as well as the entire flow behavior.

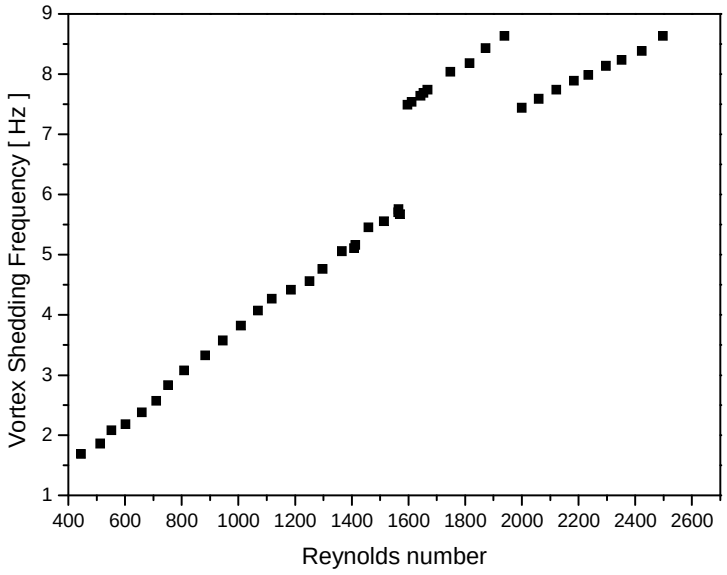

Figure 6. Reynolds number versus Vortex shedding frequency.

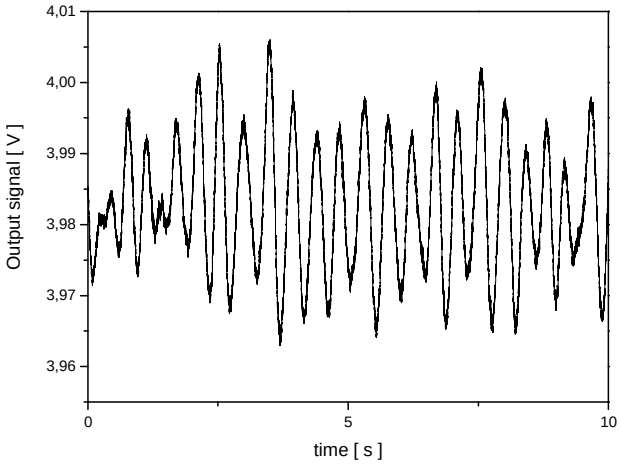

(a) Flow velocity, $Re \approx 602$.

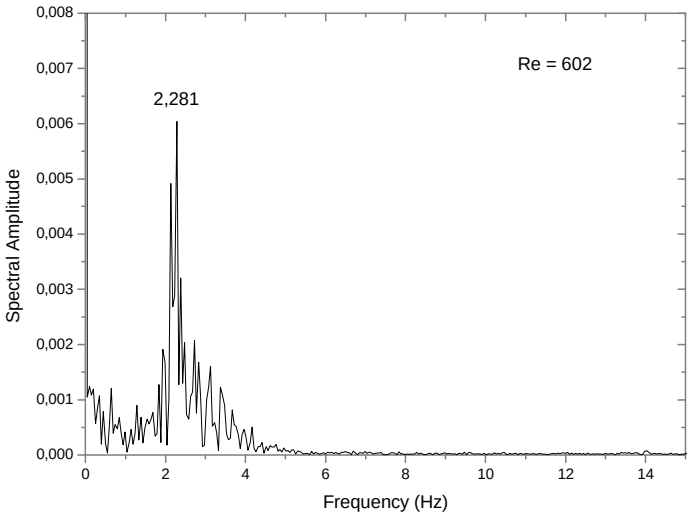

(b) Frequency spectrum, $Re \approx 602$.

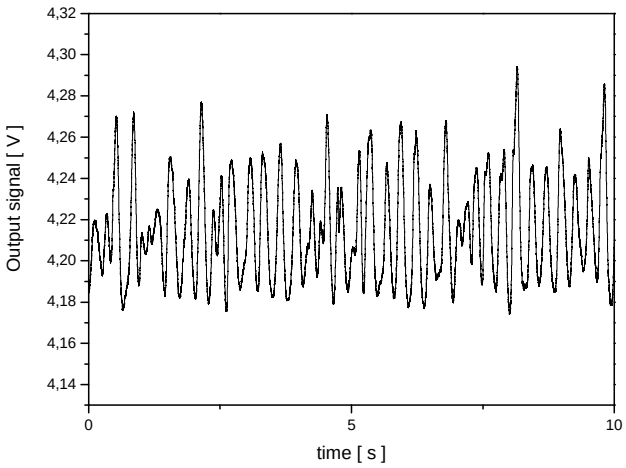

(c) Flow velocity, $Re \approx 946$.

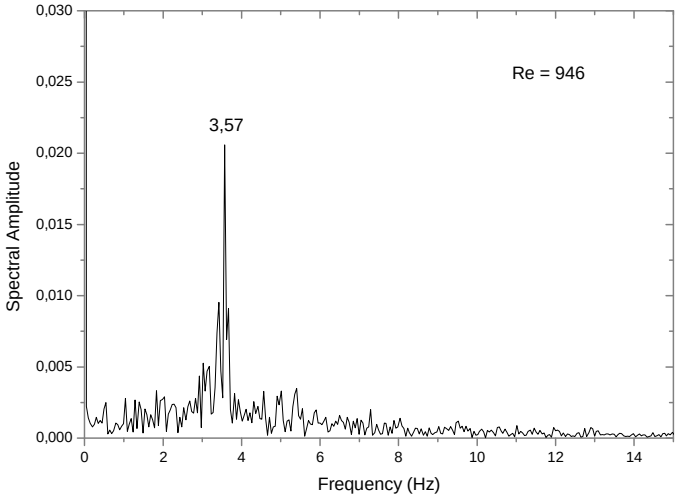

(d) Frequency spectrum, $Re \approx 946$.

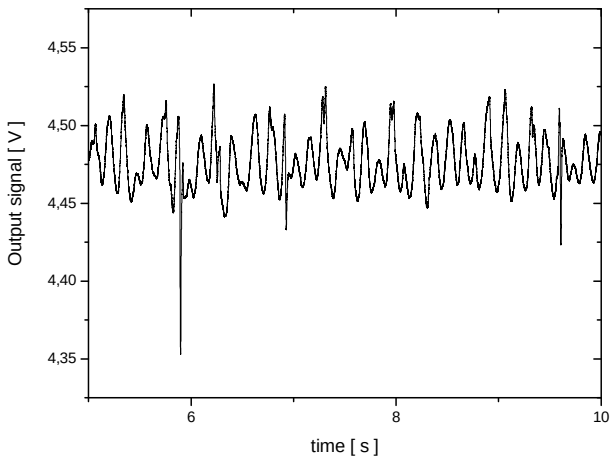

(e) Flow velocity, $Re \approx 1559$.

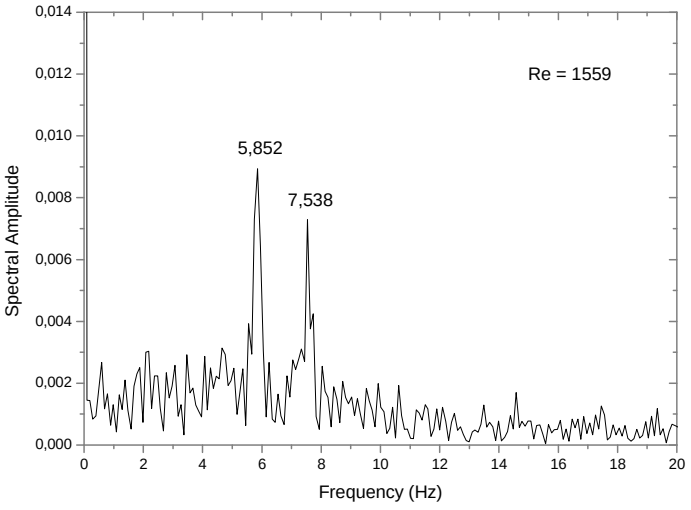

(f) Frequency spectrum, $Re \approx 1559$.

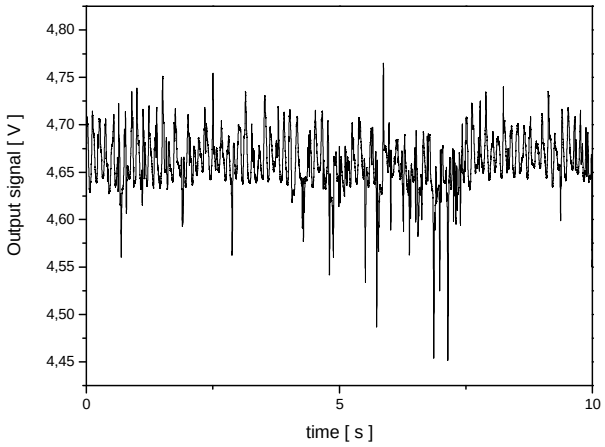

(g) Flow velocity, *Re* ≈ 1749.

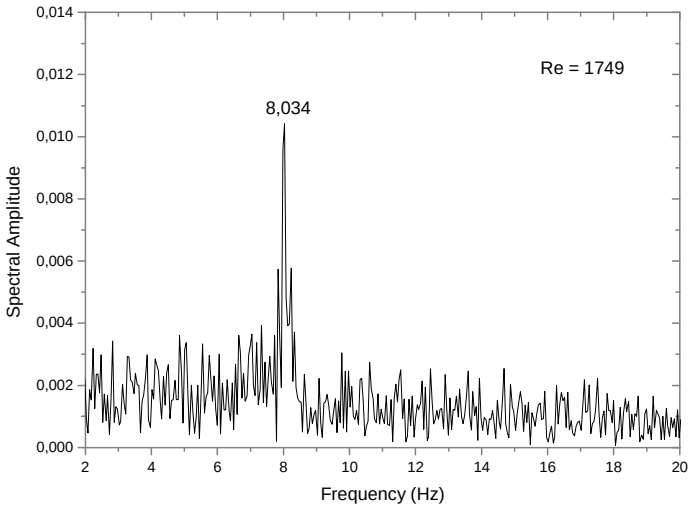

(h) Frequency spectrum, *Re* ≈ 1749.

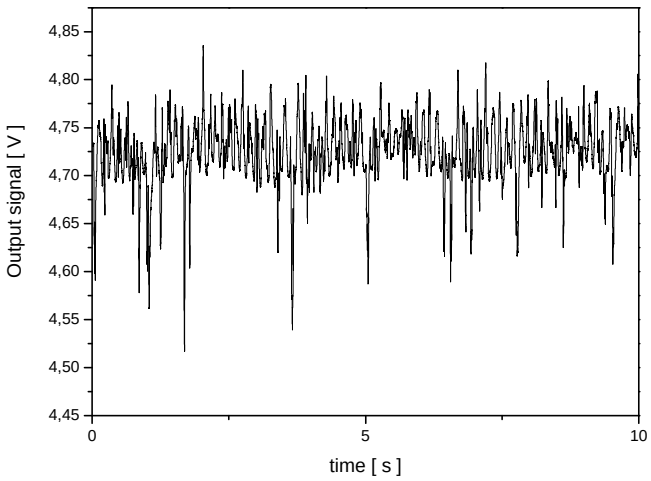

(i) Flow velocity, *Re* ≈ 2184.

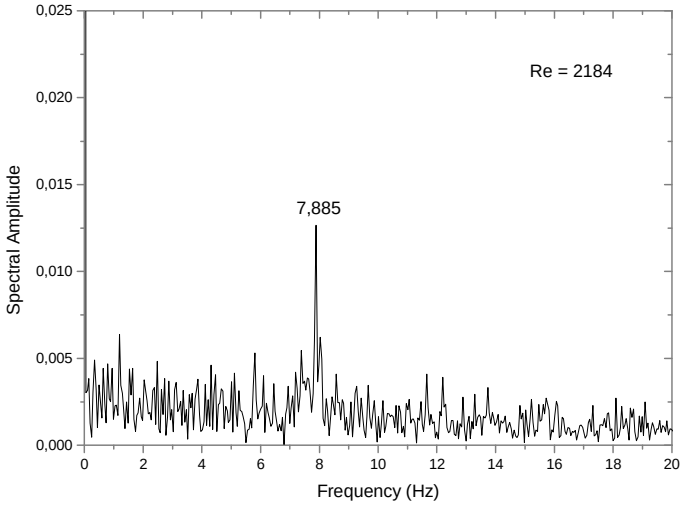

(j) Frequency spectrum, *Re* ≈ 2184.

Figure 7. Flow velocity downstream the protuberances and frequency spectrum for different Reynolds number.

4. CONCLUSION

Flow visualization has allowed putting in evidence the complex topology structures generated in the protuberances vicinity. Measurements using hot-film anemometry have permitted to obtain quantitative data about vortex shedding frequency. Combination of these two techniques is a very good way to investigate complex flows generated in a solid rough wall near the square cylindrical protuberances as made by Bassan *et al.* (2011) and Vieira and Mansur (2004). The discontinuities phenomenon depicted in Fig. 6 could not be fully investigated because of the digital video camera`s limitation of 30 fps (frames per second). New experiments are being prepared in order to study the flow pattern in this region.

5. ACKNOWLEDGEMENTS

The authors are grateful to FAPESP, CNPq, and FUNDUNESP for the financial support granted to this work.

6. REFERENCES

Bassan, R.A., Mansur, S.S. and Vieira, E.D.R., 2011. "Rebuilt of a Vertical Hydrodynamic Tunnel". 21st Brazilian Congress of Mechanical Engineering. Natal, RN, Brazil.

Bassan, R.A., Mansur, S.S., Vieira, E.D.R., 2011. "Experimental Flow Visualization Internal Channels with Wall Protuberance" (in Portuguese), proceedings of CIBEM 2011 – 10º Congresso Iberoamericano de Engenharia Mecânica, Porto, Portugal.

Clayton, B.R., Massey, B.S., 1967. "Flow Visualization in Water: A review of Techniques", Journal of Scientific Instrumentation, Vol. 44, pp. 2-11.

Freymuth, P., 1993. "Flow Visualization in Fluid Mechanics", Review Scientific Intruments, Vol. 64, pp. 1-18.

Jiménez, J., 2004. "Turbulent Flow over Rough Walls", Annu. Rev. Fluid Mech. 2004.

Merzkirch, W., 1987. "Flow Visualization", ed.2, Academic Press, Orlando.

Vieira, E.D.R., Mansur, S.S., 2004, "Visualização Experimental de Escoamentos", Coleção Cadernos de Turbulência, vol.4, Möller, S.V., Silvestrini, J.H. (eds.), pp.33-71, Associação Brasileira de Engenharia e Ciências Mecânicas - ABCM, ISBN 85-85769-19-X.

7. RESPONSIBILITY NOTICE

The authors are the only responsible for the printed material included in this paper.